IOPscience iopscience.iop.org

Home Search Collections Journals About Contact us My IOPscience

Decay dynamics of the green luminescence in Er^{3+}-doped SiN alloys

This article has been downloaded from IOPscience. Please scroll down to see the full text article.

2003 J. Phys.: Condens. Matter 15 4859

(http://iopscience.iop.org/0953-8984/15/27/317)

View the table of contents for this issue, or go to the journal homepage for more

Download details:
IP Address: 171.66.16.121
The article was downloaded on 19/05/2010 at 12:33

Please note that terms and conditions apply.

J. Phys.: Condens. Matter **15** (2003) 4859–4867 | PII: S0953-8984(03)62771-2

Decay dynamics of the green luminescence in Er^{3+}-doped SiN alloys

M J V Bell and V Anjos

Departamento de Física, Universidade Federal de Juiz de Fora, 36036-330, Juiz de Fora, MG, Brazil

E-mail: mjbell@fisica.ufjf.br

Received 28 April 2003
Published 27 June 2003
Online at stacks.iop.org/JPhysCM/15/4859

Abstract

In this paper we present results on green emission from Er^{3+}-doped amorphous SiN alloys as a function of temperature and thermal annealing. It is shown that the lifetime of the green emission from the as-deposited sample decreases by an order of magnitude as the temperature increases from 5 to 300 K. Processes such as multiphonon decay and thermalization of the $^2H_{11/2}$ and $^4S_{3/2}$ Er^{3+} levels are investigated in order to explain such behaviour. Concerning the effect of thermal annealing, our results show the activation of a new Er^{3+} site, whose nature may be related to the oxidation of the films.

1. Introduction

Several investigations have been focused on the properties of semiconductors doped with rare earths (RE). The great interest in this field is due to the fact that these ions present an optically active shell ($4f^n$) screened by outer $5s^2$ and $5p^6$ orbitals. For this reason, the luminescence resulting from radiative 4f transitions is usually sharp and independent of the temperature of the host. In particular, RE-doped wide-band-gap semiconductors have attracted considerable attention because of the interest in the electrical excitation of the 4f transitions through a carrier-mediated process. Recently, it has been demonstrated that Er^{3+} ions in GaN can generate green and infrared electroluminescence at about 550 nm and 1.5 μm, respectively [1, 2]. Red electroluminescence at 650 nm has also been reported in Pr^{3+}-doped GaN [3]. The most frequently investigated semiconductor materials including amorphous and crystalline hosts are GaN [1–3], AlN [4], GaP [5], SiN [6–9], and GaAsN [10]. The proposed applications for RE-doped wide-band-gap semiconductors in the visible range are, for example, in visible-light-emitting diodes and full colour displays [3, 6, 7].

The main advantages of Er-doped SiN thin films include a large band gap, which results in low thermal quenching [11] and compatibility of the amorphous host with silicon technology.

Notwithstanding the large number of experimental data, some processes such as activation of Er sites, effects of thermal annealing (TA), and the temperature quenching of the

0953-8984/03/274859+09$30.00 © 2003 IOP Publishing Ltd Printed in the UK

luminescence at room temperature are not completely understood. In order to discriminate among the mechanisms and features that may be responsible for this behaviour—for example, temperature dependence of the pumping efficiency, a number of optically active sites, and nonradiative processes—detailed measurements of the excitation and de-excitation of the Er^{3+} ions are required.

In this paper we present results on time-resolved green emission (due to the $^4S_{3/2} \rightarrow {}^4I_{15/2}$ transition) from Er^{3+}-doped amorphous SiN thin films as a function of temperature and thermal annealing. Such emissions are very interesting for use as probes of the Er environment due to the simple Stark multiplet structure, as compared to the $^4I_{13/2} \rightarrow {}^4I_{15/2}$ Er^{3+} transition at 1.54 μm. This is a very important characteristic when dealing with amorphous hosts, where inhomogeneous broadening prevents detailed analysis of the Stark multiplets. It is shown that the measured lifetime of the green emission decreases as the temperature increases and the effect is mainly attributed to thermalization of the $^2H_{11/2}$ and $^4S_{3/2}$ Er^{3+} levels. Our results also indicate that at least two classes of Er^{3+} centres are present in the SiN films. One may be activated by the TA, and presents a short lifetime (at about 0.4 μs) and higher luminescence intensity. The other is longer-lived (540 μs), and is dominant in the as-deposited (AD) sample.

2. Experimental set-up

Er-containing amorphous silicon nitride samples were deposited at room temperature by rf sputtering. The samples were subjected to TA. The isochronal thermal anneals (15 min each) were cumulative, and performed in a temperature-controlled furnace at atmospheric pressure. The samples used in the present work are those called sample D in [7]. One is the AD sample and the others were annealed at 300, 900, and 1050 °C. The nitrogen content in the a-SiN resulted in almost stoichiometric films, with [N] estimated to be 50 at.%. The atomic Er concentration is 0.5%, in accordance with Rutherford backscattering spectroscopy results. Time-resolved visible measurements were achieved using a coumarin dye laser pumped by a pulsed N_2 laser. The pulse width was 10 ns and the repetition rate was fixed at 10 Hz. The pumping wavelength was resonant with the $^4I_{15/2} \rightarrow {}^2H_{11/2}$ Er^{3+} transition, at 520 nm. The luminescence emission was dispersed by a triple monochromator (SPEX 1403) and acquired by an OMA system (optical multichannel analyser). The acquisition gate was varied from 100 ns to 50 μs. The delay varied in the range from 0 to 2000 μs. The triggering signal was achieved from a silicon photodiode, with the time response of 100 ps. The system response was estimated to be 10 ns.

All measurements were performed either at room temperature in air or in a liquid-He cryostat (JANIS), in which the temperature could be tuned between 5 and 300 K.

3. Results

Figure 1 presents the Er^{3+} levels. Er^{3+} has a ground [Xe] $4f^{11}$ electronic configuration, and the excited states are given according to the Diecke convention, $^{2S+1}L_J$ [12]. The energy gap of the a-SiN thin films is 3.9 eV ($\sim$31 000 cm^{-1}) for the E_{03}-gap and 5.1 eV ($\sim$41 000 cm^{-1}) for the E_{04}-gap, where E_{03} (E_{04}) means the energy at which the absorption coefficient reaches 10^3 cm^{-1} (10^4 cm^{-1}) [7]. The arrow indicates the pumping energy used in the experiment, resonant with the $^4I_{15/2} \rightarrow {}^2H_{11/2}$ transition.

Figure 2 shows the time-resolved photoluminescence emissions in the green spectral region for the AD sample, at 5 K for different delays. The gate was 50 μs and the delay varied from 0 to 2000 μs. The luminescence is characterized by two bands centred at 549

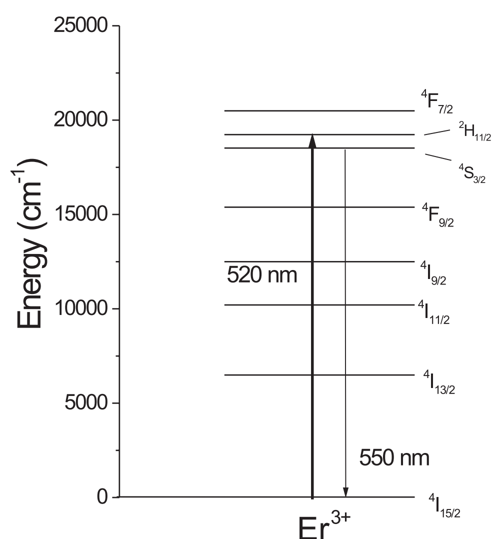

Figure 1. Er^{3+} energy levels.

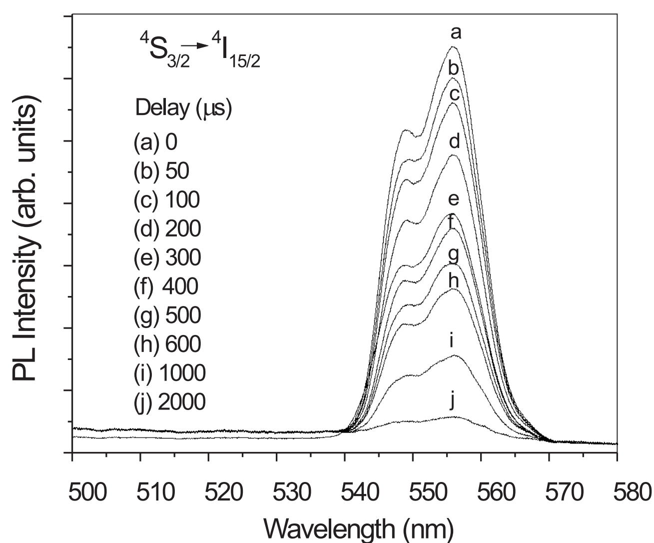

Figure 2. Time-resolved green emission, corresponding to the $^4S_{3/2} \rightarrow {}^4I_{15/2}$ Er^{3+} transition, for the AD sample at 5 K.

and 556 nm, ascribed to the $^4S_{3/2} \rightarrow {}^4I_{15/2}$ Er^{3+} transition. Crystalline fields due to the local environment, especially the nearest-neighbouring atoms, determine the Stark splitting of the Er^{3+} levels. Previous studies of RE ions in amorphous hosts have shown that due to the low point symmetries of the sites occupied by RE ions, the manifolds of the ions usually have full splitting $(2J + 1)$ [13]. In particular, the $^4S_{3/2}$ level $(J = 3/2)$ has twofold degeneracy and the recombination with the fundamental state $^4I_{15/2}$, with eight Stark sublevels, would result in a maximum number of 16 lines. Nevertheless, due to the substantial inhomogeneous broadening of the amorphous host, some of the expected spectral lines are mixed and make the

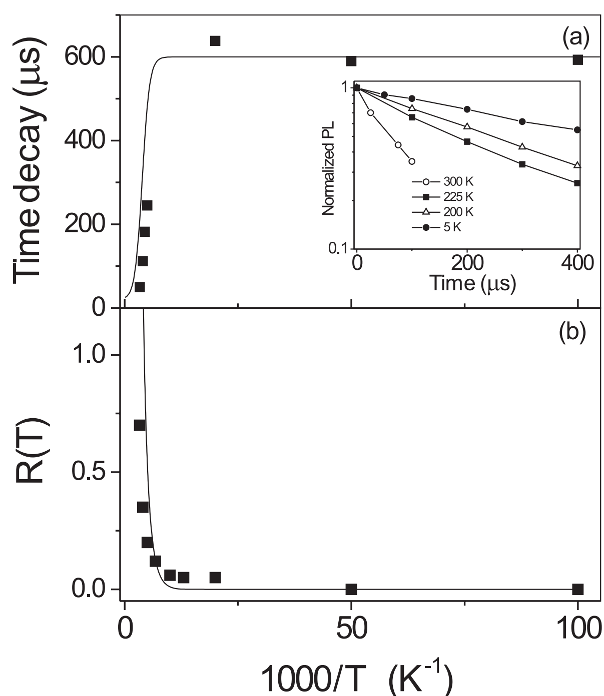

Figure 3. (a) Lifetimes of the $^4S_{3/2} \rightarrow {}^4I_{15/2}$ Er^{3+} transition, for the AS sample, as a function of temperature. The continuous curve resulted from fitting procedures using equation (1). The inset indicates some selected decay curves on a semilog scale. (b) The ratio $R(T)$ of the intensities of the $^2H_{11/2} \rightarrow {}^4I_{15/2}$ and $S_{3/2} \rightarrow {}^4I_{15/2}$ Er^{3+} transitions, as a function of temperature. The continuous curve resulted from fitting procedures using equation (4).

number of observable lines less than the number of expected spectral lines [14]. In our case, the inhomogeneous broadening results in two observed structures, centred at 549 and 556 nm. The luminescence decay was fitted by an exponential function given a lifetime of 540 μs. It is important to note that the emission due to the $^2H_{11/2} \rightarrow {}^4I_{15/2}$ transition is not seen at this temperature. The photoluminescence of the SiN host is superimposed on the Er^{3+} emission, but it is not seen in figure 2 because its lifetime is about 10 ns and it is not detectable in the time range used in the present work (from 100 ns to 2 ms).

Figure 3(a) shows the measured time decays of the $^4S_{3/2}$ level as a function of temperature for the AS sample. The temperature dependence of the lifetime was monitored at 550 nm. The lifetime varied from 540 μs at 5 K to 50 μs at room temperature. The inset shows some selected decay curves on a semilog scale. Figure 3(b) shows the ratio $R(T)$ of the PL intensities of the $^2H_{11/2} \rightarrow {}^4I_{15/2}$ and $^4S_{3/2} \rightarrow {}^4I_{15/2}$ Er transitions. The continuous lines in figures 3(a) and (b) resulted from fitting procedures to be discussed in the next section.

Figure 4 exhibits the time-resolved spectra at 5 K in the green spectral region for a sample subjected to thermal annealing at 900 °C. It can be noted that the lineshape is composed of two structures, one peaked at 544 nm, and a shoulder at about 554 nm. Clearly, the lineshape is different from that of the AD sample. Moreover, the total average energy of the $^4S_{3/2}$ level is shifted to higher values compared to that for the AD sample. This may be attributed to the change of the ligand field (or equivalently the chemical environment) of the Er ions during the TA. The inset shows the intensity decay at 550 nm, as a function of time. The points were fitted by an exponential decay and the lifetime achieved was 0.4 μs.

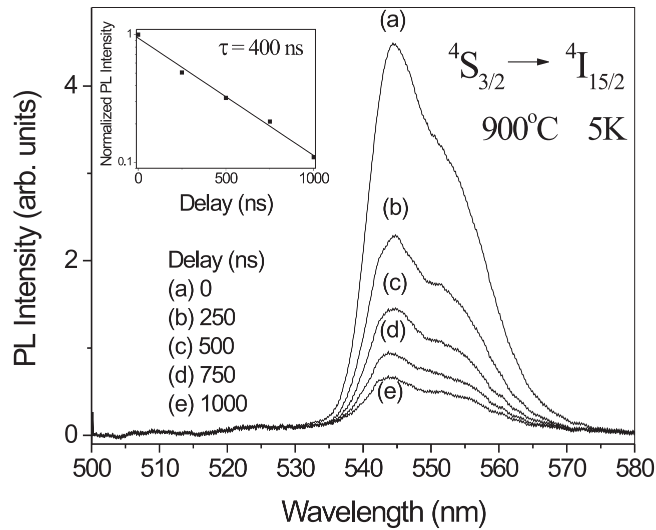

Figure 4. Time-resolved green spectra for the sample subjected to TA at 900 °C, monitored at 5 K.

4. Discussion

An Er^{3+} ion in an excited state decays with a measured lifetime τ determined by the radiative and nonradiative decay rates (W_{rad} and W_{nrad}, respectively), according to the following equation:

$$\frac{1}{\tau} = W_{rad} + W_{nrad}. \quad (1)$$

The most important nonradiative processes to be considered are:

(a) multiphonon decay, which depends basically on the energy gap from the low-lying energy level, host phonon energy, and temperature;
(b) (b) energy transfer among Er ions (as cross-relaxation and energy migration) or mediated by the semiconductor host.

These may be resonant (temperature independent) or assisted by phonons [15]. Considering that the Er concentration is low, energy transfer among Er ions can be neglected and only multiphonon relaxation (W_{mp}) needs to be considered. The most common expression for W_{mp} is [16]

$$W_{nrad} = W_{mp} = C \exp(-\alpha\, \Delta E_0)[1 - \exp(-h\omega_p/kT))]^{-p} \quad (2)$$

where ΔE_0 is the energy gap between the $^4S_{3/2}$ and $^4F_{9/2}$ levels (2800 cm^{-1}, from figure 1), p is the number of phonons needed to bridge the gap, and $h\omega_p$ is the phonon energy of the host. C and α are host-dependent parameters, and are determined by the fitting procedures. $h\omega_p$ is about 500 cm^{-1} from Raman measurements on similar samples and, consequently, p is equal to 6 [17].

As regards the radiative rate of the $^4S_{3/2}$ level, it should be noted that it may depend on temperature, because of the thermalization of the $^2H_{11/2}$ level. This is corroborated by the PL behaviour of the green emission as the temperature decreases. Clearly, the $^2H_{11/2} \rightarrow {}^4I_{15/2}$ band disappears as the temperature goes to 5 K, indicating that the main pumping channel of the $^2H_{11/2}$ was from the $^4S_{3/2}$ level. Such behaviour has been reported for several Er-doped

Table 1. Comparison among the time decays of the $^4S_{3/2} \rightarrow {}^4I_{15/2}$ Er^{3+} transition (τ) for different hosts. T is the temperature; λ corresponds to the excitation wavelength.

Host	Er concentration (%)	τ (μs)	λ (nm)	T (K)	References
GaN	1	5	537	300	[18]
ZnO	5	4.3	488	300	[33]
Silicate	—	0.7	488	300	[33]
ZBLAN		356	488	300	[33]
SiN (AD)	0.5	540	520	5	This work
		50	520	300	
SiN (TA: 900 °C)	0.5	0.4	520	5	This work

glasses and recently for Er-doped GaN [18] and SiN thin films [7]. In this case, the effective radiative transition probability of the two levels can be obtained from the expression [15]

$$W_{rad} = \frac{1/\tau_{550} + (4/\tau_{520}) \exp[-\Delta E/kT]}{1 + 4 \exp[-\Delta E/kT]} \tag{3}$$

where τ_{550} and τ_{520} stand for the intrinsic radiative lifetime of the $^4S_{3/2}$ and $^2H_{11/2}$ levels, respectively, and ΔE stands for their energy gap. From figure 1, ΔE is estimated to be in the range from 700 to 900 cm^{-1}.

The continuous line in figure 3(a) represents the fitting by means of equation (1). The model reproduces satisfactorily the experimental points and indicates that the multiphonon decay is very slight, as the constant $C \exp(-\alpha\, \Delta E)$ is given by 170 s^{-1}. The other parameters obtained by the fitting are $\tau_{550} = 600\ \mu$s, $\tau_{520} = 20\ \mu$s, and $\Delta E = 750$ cm^{-1}. Note that the former should be similar to the lifetime measured for the $^4S_{3/2}$ level at 5 K, while the latter is a fitting parameter, since the $^2H_{11/2}$ lifetime at 5 K without thermalization (the intrinsic $^2H_{11/2}$ lifetime) cannot be measured. In order to verify the validity of the parameters obtained, figure 3(b) shows the ratio $R(T)$ of the PL intensities of the $^2H_{11/2} \rightarrow {}^4I_{15/2}$ and the $^4S_{3/2} \rightarrow {}^4I_{15/2}$ Er transitions. If thermalization is the unique pumping channel for the $^2H_{11/2}$ level, such relation must be given by

$$R(T) = \frac{\tau_{550}}{\tau_{520}} \frac{E_H}{E_S} \frac{g_H}{g_S} \exp[-\Delta E/kT] \tag{4}$$

where E_H (E_S) is the energy of the $^2H_{11/2} \rightarrow {}^4I_{15/2}$ ($^4S_{3/2} \rightarrow {}^4I_{15/2}$) transition and g_H (g_S) corresponds to the $^2H_{11/2}$ ($^4S_{3/2}$) degeneracy. The continuous line in figure 3(b) shows the simulation of equation (4), with the same parameters as were used in the fitting of figure 3(a). On can note a small deviation from the fitting at temperatures near 300 K. Such an effect is attributed to the possible energy transfer between the host and the Er ions [6].

In view of the results revealed, it is suggested that the temperature quenching of the photoluminescence emission in the AD a-SiN sample is mainly due to thermalization of the $^4S_{3/2}$ and $^2H_{11/2}$ Er^{3+} levels.

For comparison purposes, table 1 shows other time decays reported in the literature for the $^4S_{3/2} \rightarrow {}^4I_{15/2}$ Er^{3+} transition in different hosts. The determination of the lifetime is important for establishing the performance characteristics of future devices based on Er-doped semiconductors. It determines, for example, the modulation bandwidth of optoelectronic devices. In this sense, shorter lifetimes are indicated for high-frequency response, while longer lifetimes limit the operation to CW devices.

The lifetime of the $^4S_{3/2} \rightarrow {}^4I_{15/2}$ Er^{3+} transition for the sample subjected to TA at 900 °C indicated a time decay of about 0.4 μs at 5 K. The measured lifetime is about three orders of magnitude shorter than that in the AD sample. It was also found that the green emission

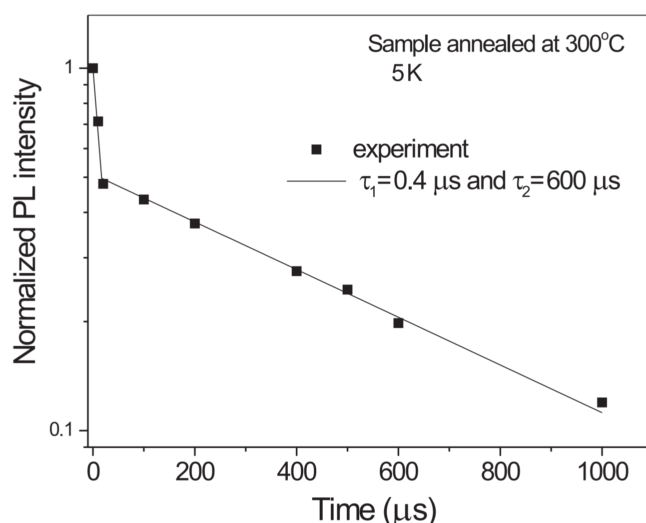

Figure 5. The intensity decay of the $^4S_{3/2} \rightarrow {}^4I_{15/2}$ Er^{3+} transition, for the sample subjected to TA at 300 °C, monitored at 5 K.

(at room temperature) increased with the temperature of annealing, at least up to the maximum temperature of the experiment, 1050 °C [7].

It is currently believed that TA may induce the following processes: (a) reduction of nonradiative centres, (b) structural rearrangement of the host, and (c) optical activation of Er sites. It is important to note that such effects are not mutually exclusive and may occur simultaneously.

Process (a) would result in the reduction of nonradiative rates, and, consequently, in longer lifetimes. However, the experimental results indicate a shorter lifetime for the thermally annealed sample [7]. Statement (b) indicates that the infrared and Raman spectra of the samples deserve detailed analysis. The main features previously reported by us in [7] are the following:

(1) Infrared spectra of the AD and annealed samples are significantly different. It was shown that as the temperature of the TA is increased, a band centred at about 1080 cm^{-1} appears. This band was attributed to the stretching mode of the Si–O ligands and it is originated from the oxidation of the sample.
(2) The Si–N ligands remained unchanged during TA. So we believe that nitrogen makes no significant contribution to the process.
(3) The Si–O ligands (figure 5 of [7]) and PL intensity of the $^4S_{3/2}$ level (figure 7(a) [7]) exhibit similar increases with the temperature of annealing. This behaviour suggests that oxygen may play an important role during the TA process.

Andrés *et al* [25] reported that the peak position of the main Si–O–Si stretching band as a function of the TA temperature in amorphous SiO_x films is progressively shifted to the SiO_2 value, at 1080 cm^{-1}. This peak centre position is near to the one that we found for our sample. Moreover, it is well known that the oxidant species may diffuse towards the SiN/oxide interface and react with the silicon nitride [19–24]. Such an effect may result in the presence of interstitial O atoms or the conversion of SiN to SiO_2 [19, 23]. In this sense, there has also been reported evidence for the presence of isolated oxide and nitride substructures [19, 24]. So, it is very plausible that the oxidation of the sample results in changes in the local surroundings of

the Er^{3+} ions—even in the formation of an O-interstitial-rich environment or in the formation of SiO_2 substructure.

Several authors have reported that O codoping increases the PL emission of the $^4I_{13/2} \rightarrow {}^4I_{15/2}$ Er^{3+} transition at 1.54 μm and can induce activation of other Er sites [26–31]. Przybylinska *et al* [27] reported finding optically active Er^{3+} centres of different kinds in Si coimplanted with C, N, and O, with symmetry lower than the site symmetry of Si in crystalline Si. Moreover, Coffa *et al* [26] have shown that the presence of oxygen strongly increases the photoluminescence intensity of the $^4I_{13/2} \rightarrow {}^4I_{15/2}$ Er^{3+} transition. Michel *et al* [32] have provided evidence that the reaction occurring between Er and O during annealing at around 900 °C was very effective in enhancing the photoluminescence of Er in Czochralski-grown Si.

On the basis of the experimental data, the following picture can be proposed. At least two different classes of optically active Er^{3+} site exist in the a-SiN films, characterized by different $^4S_{3/2} \rightarrow {}^4I_{15/2}$ lineshapes and lifetimes. One of these sites is present in the AD sample and decays with a long lifetime (540 μs). When the sample is subjected to thermal annealing, the contribution of this site vanishes. The other Er^{3+} site decays with a short lifetime (0.4 μs), and it can be activated by the TA. We propose that TA, which results in increase in the number of Si–O ligands, modifies the local surroundings of Er^{3+} ions in the amorphous SiN thin film, resulting in an oxygen-rich environment for Er^{3+} ions. As oxygen has high electronegativity, it provides a more ionic environment for Er ions, which has been observed to be favourable for activation of Er sites [11, 34, 35]. Additional support for this statement is given by the shift to higher energies of the $^4S_{3/2} \longrightarrow {}^4I_{15/2}$ emission in the annealed sample. According to the theory of RE radiative transitions developed by Judd and Ofelt [13], the increase in the ionicity of the environment results in a blue-shift of the Stark levels, due to the increase of the local field. Moreover, the relaxation of the selection rules induced by the more intense local field in the ionic environment results in shorter lifetimes. This is in accordance with our results, because the lifetime for the annealed sample is shorter than that for the AD sample and the luminescence emission is more intense in the annealed sample.

In order to verify the transition in terms of Er sites going from as-deposited samples to annealed samples, we have also measured the decay time of the $^4S_{3/2}$ level at 5 K for the sample annealed at 300 °C. In this case, the decay curve is characterized by a double-exponential decay. The experimental decay was fitted with two decay times: 0.4 and 600 μs (dotted line), which correspond to the lifetimes of the two Er sites detected in the amorphous SiN samples.

5. Conclusions

The present paper presented results on the green emission of Er^{3+}-doped amorphous silicon nitride as a function of temperature and TA. It was shown that the temperature dependence of the green emission reflects the thermalization of the $^2H_{11/2}$ and $^4S_{3/2}$ Er^{3+} levels. It was also demonstrated that thermal annealing resulted in the activation of a new Er site, characterized by stronger green emission and shorter lifetime than for the Er site found in the AD sample. It was suggested that the Er activation is related to the oxidation of the samples during the TA.

Acknowledgments

This work was partially supported by the Brazilian Agencies Capes, CNPq and FAPESP.

References

[1] Steckl A J, Garter M, Birkhahn R and Scofield J 1998 *Appl. Phys. Lett.* **73** 2450
[2] Torvik J T, Qiu C H, Feuerstein R J, Pankove J I and Namavar F 1997 *J. Appl. Phys.* **81** 6343
[3] Birkhahn R, Garteer M and Steckl A J 1999 *Appl. Phys. Lett.* **74** 2161

[4] Wu X, Hömmerich U, Mackenzie J D, Abernathy C R and Pearton S J 1997 *Appl. Phys. Lett.* **70** 2126
[5] Wang X Z and Wessels B W 1994 *Appl. Phys. Lett.* **65** 584
[6] Bell M J V, Nunes L A O and Zanatta A R 1999 *J. Appl. Phys.* **86** 338
[7] Zanatta A R, Bell M J V and Nunes L A O 1999 *Phys. Rev.* B **59** 10091
[8] Zanatta A R and Ribeiro C T M 2001 *Appl. Phys. Lett.* **79** 488
[9] Bell M J V and Anjos V 2003 *Physica* E **17** 137
[10] Zanatta A R 2000 *J. Non-Cryst. Solids* **266** 854
[11] Favennec P N, Haridon H L, Moutonnet D, Salvi M and Le Guillou Y 1989 *Electron. Lett.* **25** 718
[12] Diecke G H 1968 *Spectra and Energy Levels of Rare-Earth Ions in Crystals* (New York: Wiley–Interscience)
[13] Judd B R 1962 *Phys. Rev.* **127** 750
Ofelt G S 1962 *J. Chem. Phys.* **27** 511
[14] Desurvire E and Simpson J R 1990 *Opt. Lett.* **15** 547
[15] Shinn M D, Sibley W A, Drexhage M G and Brown R N 1983 *Phys. Rev.* B **27** 6635
[16] Layne C B, Lowdermilk W H and Weber M J 1977 *Phys. Rev.* B **16** 10
[17] Giorgis F, Pirri C F, Tresso E, Rigato V, Zandolin S and Rava O P 1997 *Physica* B **229** 233
[18] Hömmerich U, Seo J T, Abernathy C R, Steckl A J and Zavada J M 2001 *Mater. Sci. Eng.* B **81** 116
[19] Carrillo-López J and Morales-Acevedo A 1997 *Thin Solid Films* **311** 38
[20] Schalch D, Sharmann A and Wolfrat R 1987 *Thin Solid Films* **155** 301
[21] Lee S H, Rixecker G, Aldinger F, Choi S C and Auh K 2003 *J. Eur. Ceram. Soc.* **23** 1199
[22] Gregory O J and Richman M H 1982 *Thin Solid Films* **91** 163
[23] Galanov B A, Ivanov S M, Kartuzov E V, Kartuzov V V, Nickel K G and Gototsi Y G 2001 *Comput. Mater. Sci.* **21** 79
[24] Banerji N, Serra J, Gonzalez P, Chiussi S, Parada E, Leon B and Perez-Amor M 1998 *Thin Solid Films* **317** 214
[25] Andrés E S, del Prado A, Martil I, Gonzalez Diaz G, Martinez F L, Bravo D and López F J 2002 *Vacuum* **67** 531
[26] Coffa S, Franzo G, Priolo F, Polman A and Serna R 1994 *Phys. Rev.* B **49** 16313
[27] Przybylinska H, Hendorfer G, Bruckner M, Palmetshofer L and Jantsch W 1995 *Appl. Phys. Lett.* **66** 490
[28] Takahei K and Taguchi A 1993 *J. Appl. Phys.* **74** 1979
[29] Uekusa S, Uchika K and Kumagai M 1999 *Physica* B **273/274** 778
[30] Nakashima K, Eryu O, Iioka O, Nakata T and Watanabe M 1997 *Nucl. Instrum. Methods Phys. Res.* B **127/128** 475
[31] Uekusa S, Yano Y, Fukaya K and Kumagai M 1997 *Nucl. Instrum. Methods Phys. Res.* B **127/128** 541
[32] Michel J, Benton J L, Ferrante R F, Jacobson D C, Eaglesham D J, Fitzgerald E A, Xie Y H, Poate J M and Kimerling L C 1991 *J. Appl. Phys.* **70** 2672
[33] Kohls M, Bonanni M, Spanhel L, Su D and Giersig M 2002 *Appl. Phys. Lett.* **81** 3858
[34] Polman A 1997 *J. Appl. Phys.* **82** 1
[35] Zanatta A R and Freire F L 2000 *Phys. Rev.* B **62** 2016